JOURNAL OF MATERIALS SCIENCE 32 (1997) 6107–6117

Statistical analysis of failure of SiC fibres in the presence of bimodal flaw populations

N. LISSART, J. LAMON
Laboratoire des Composites Thermostructuraux, UMR 47 (CNRS-SEP-UB1), Domaine Universitaire, 3 allée de La Boëtie 33600 Pessac, France

Statistical parameters pertinent to silicon carbide fibres were estimated from experimental distributions of failure data (including strengths and strains) using the linear regression and maximum likelihood estimators. Strengths were evaluated using the average diameters of fibres, diameters at failure locations measured by SEM, and taking into account the diameter variations along the fibre axis, as evidenced by laser diffractometry. It was shown that gauge-length insensitive statistical parameters were estimated when considering that fibre fracture was dictated by two populations of partially concurrent flaw populations, including intrinsic and extrinsic flaws.

1. Introduction

The mechanical behaviour of composite materials is strongly influenced by the failure of the reinforcing fibres. Ceramic fibres exhibit a significant scatter in failure properties as a result of the presence of randomly distributed fracture inducing microstructural flaws. The criticality of these flaws is determined by several factors, including their nature, geometry, dimensions and location, and orientation with respect to the stress field. The well-known Weibull's model [1] is the most widely used for the description of the statistical distribution of failure strengths of fibres under uniaxial stress states.

Most authors assume the presence of a single population of volume-located fracture-inducing flaws [2–5]. Failure probability under uniform uniaxial tensile stresses is given by the following equation

$$P = 1 - \exp\left[- V \left(\frac{\sigma}{\sigma_{0v}} \right)^{m_v} \right] \qquad (1)$$

where m_v is the shape parameter (often referred to as Weibull modulus), σ_{0v} is a scale factor, V is the volume under stresses and σ is the applied stress field. m_v reflects the scatter in strength data and σ_{0v} is somewhat related to the average fracture strength.

The two adjustable statistical parameters of the Weibull distribution (m_v and σ_{0v}) are derived from fracture data using an estimator. An estimator is a method or algorithm to fit the distribution to the experimental data. Methods used for such estimators include linear regression, maximum likelihood, moments methods, etc.

The distribution's parameters are useful for predicting fibre failure under various loading geometries, as involved in different stress states, in fibre bundles, or in fibre-reinforced composites. Therefore, determination of the true statistical parameters is required for failure prediction purposes.

Various estimates of the Weibull modulus for Nicalon SiC fibres have been published in the literature (see, for instance [6] and references therein). The data indicate a wide variability in the reported Weibull moduli: $m \approx 2.3$–5.3. The scale factor is generally not estimated.

Estimation of statistical parameters is not easy in most cases, and particularly so for the SiC fibres. Thus, inspection of the Weibull plots of strength data measured on fibres having various gauge lengths often reveals the presence of several families of data [7–11]. Authors have identified bimodal populations of fracture inducing flaws located in the surface and in the volume of fibres and acting concurrently [7–11]. Failure probability is derived from the product of survival probabilities from each population. A few authors have introduced an arbitrary coefficient in the Weibull equation ($0 < \alpha < 1$) in order to correct the dependence of statistical parameters on the gauge lengths and the resulting failure predictions [12, 13].

Additional factors may affect the statistical parameters estimates. Thus, certain fibres, such as the SiC fibres (Nicalon), possess a non-constant diameter or a non-circular cross-section. Therefore, a satisfactory measure of the cross-sectional area is not available for derivation of the fracture strengths from the applied forces. Furthermore, the stress state acting on the fibre is not uniform, although uniaxial stresses were applied uniformly at fibre ends. Finally, the method of fitting Equation 1 to experimental strength data has also been shown to affect the statistical parameters estimates [14–17].

The main objective of the present work was to investigate the influence of such factors upon the statistical parameters estimates, in order to determine the most appropriate ones for failure predictions of fibre bundles and of ceramic matrix composites. The analysis focused on Nicalon fibres which are introduced in

0022–2461

various composites. The goodness-of-fit of the Weibull distribution to the experimental failure data was assessed using the Andersson–Darling test [18], which is considered as the most powerful of the empirical distribution function tests [19]. This test is based upon determination of the area of discrepancy between the plot of experimental data and the calculated distribution of failure data; it gives more importance to the tails of the distribution and is the most appropriate for small samples.

The statistical parameters were estimated using the methods of linear regression and maximum likelihood. The following cases were examined: (i) failure was characterized either by a stress or by a strain; (ii) failure strengths were calculated from various estimates of the fibre diameter – the average value, the diameter at the location of failure, or diameters varying along the fibre, (iii) various populations of fracture-inducing flaws were considered – a single population, then two concurrent populations of surface- and volume-located flaws, and finally partially concurrent populations of intrinsic and extrinsic flaws.

2. Determination of statistical distributions of failure data

2.1. Tensile tests

Three batches of about 30 test specimens were prepared from a single spool of 500 filament tow of silicon carbide (Nicalon NL 202). Suitable lengths of bundles were cut to obtain test specimens having, respectively, a 25, 50 and 75 mm gauge length. The sizing was removed using a solvent.

The single filaments were tested under tension for measurement of fibre elongation and of the associated force at failure. The conventional "window card" technique was used. Tensile tests were carried out on a specific tensile machine for fibre testing. A constant cross head speed was applied such that the deformation rate was 1% min^{-1}. Strains were derived from crosshead displacement measured using a LVDT extensometer mounted on the grips. A layer of grease was deposited on the fibres to obtain the fibre fragments after testing for fractographic examination of fractured surfaces using the scanning electron microscope (SEM). 75% of the fibre test specimens were examined by SEM.

2.2. Fibre diameter measurement

Fibre diameters were measured by laser diffractometry prior to tensile testing. Interaction of a laser beam with the fibre under the so-called Fraunhoffer diffraction conditions, provides a diffraction pattern [20]. Filament diameter is derived from fringe spacing measurement. Diameter was measured every 5 mm along the fibre axis. The average of all the diameters obtained by laser diffractometry was 14.5 μm (standard deviation 2 μm).

Fibre diameter at the failure location (referred to as d_{SEM}) was measured by SEM.

Fig. 1 examplifies the diameter variations detected on single fibres. Fig. 2 indicates a rather large scatter

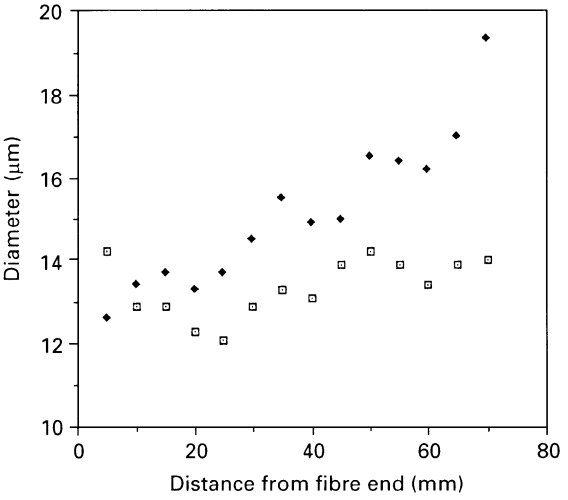

Figure 1 Examples of diameter variations detected by laser diffractometry in two Nicalon fibres with a 75 mm gauge length.

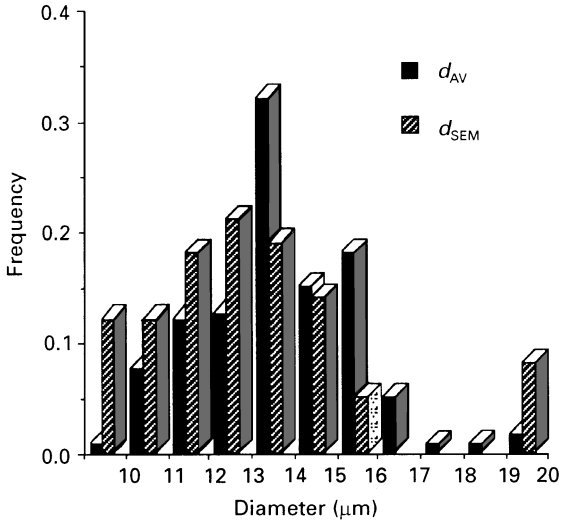

Figure 2 Histogram of the diameters measured on Nicalon fibres.

in the mean diameters measured on each fibre by laser diffractometry (referred to as d_{av}), and in d_{SEM}. As shown in Table I, diameters at failure locations were significantly smaller than the mean values, d_{av}, measured by laser diffractometry.

2.3. Determination of statistical distributions of failure data

Failure stresses were derived from the forces measured at fracture and from fibre cross-sectional areas estimated:

(i) from the average diameters measured on each fibre using laser diffractometry

$$\sigma^i_{d_{AV}} = \frac{4F^i_r}{\pi(d^i_{AV})^2} \quad (2)$$

where F^i_R is the force at failure for the ith fibre;

(ii) from the diameters at failure locations measured using SEM

$$\sigma^i_{d_{SEM}} = \frac{4F^i_r}{\pi(d^i_{SEM})^2} \quad (3)$$

TABLE I Mean diameters measured by laser diffractometry, ($\bar{d}_{AV}$, and by scanning electron microscopy, $\bar{d}_{SEM}$. Standard deviations are given in parentheses

Gauge length (mm)	$\bar{d}_{AV}$ (μm)	$\bar{d}_{SEM}$ (μm)
25	14.7	13.76
	(1.9)	(2.25)
50	14.8	13.05
	(1.2)	(1.48)
75	14.3	12.81
	(2.3)	(1.71)

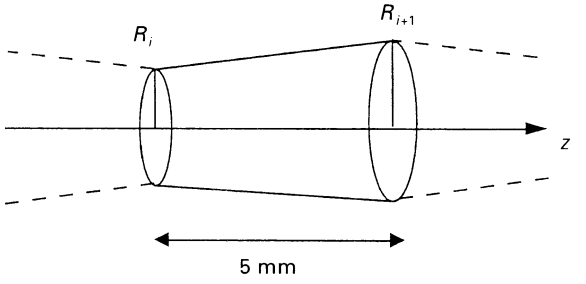

Figure 3 Schematic diagram showing the description of fibre diameter variations by truncated cones.

(iii) considering the diameter changes as evidenced by laser diffractometry. The fibre was assimilated to a chain of truncated cones with a radius varying linearly between R_i and R_{i+1}, and with a height of 5 mm according to the steps selected for diameter measurement (Fig. 3). The failure stress refers to the maximum stress acting on the fibre, which corresponds to the smallest diameter measured along this fibre (d^i_{min})

$$\sigma^i_{d_{min}} = \frac{4F^i_r}{\pi(d^i_{min})^2} \quad (4)$$

Strains to failure were derived from elongations at fracture.

The associated probabilities of failure, P_i, were deduced using ranking statistics. Ordering the failure data from smallest to largest and assigning a ranking number i, the probabilities of failure were then assigned by the following relationship

$$P_i = \frac{i - 0,5}{N} \quad (5)$$

where N is the total number of specimens.

Several other relationships are available to assign probabilities, but the one defined in Equation 5 is preferred because it yields small statistical bias errors in the resulting statistical parameters [14].

2.4. Estimation of statistical parameters

The conventional Weibull linear regression estimator involves regression of a transformed probability term, $\ln\ln(1/1 - P_i)$, on a transformed fracture strength term, $\ln\sigma_i$.

The slope of the linear regression line provides an estimate of the Weibull modulus, whereas the intercept is used to estimate the second parameter, σ_{0v}, according to the following transformed failure probability equation derived from Equation 1

$$\ln[-\ln(1 - P_i)] = \ln V + m_v\ln\sigma_i - m_v\ln\sigma_{0v} \quad (6)$$

The maximum likelihood approach for estimating the adjustable statistical parameters is well-developed and well-respected by the statistical community [14]. It has been proven in the statistical literature that the parameters resulting in the maximum value of the likelihood are very good estimates of the true parameters [14]. The mathematics used in derivation of a maximum likelihood estimator and the iterative process used in executing the estimator are merely the means of finding parameters to maximize the likelihood, or usually in practical evaluation, the log-likelihood. The maximum likelihood estimate of the Weibull modulus, m, is evaluated by iteratively determining the value of m that satisfies Equation 7. After m is known, the second Weibull parameter, σ_0, is determined from Equation 8

$$\frac{N}{m_v} + \sum_{i=1}^{N}\ln(\sigma_i) - N\frac{\sum_{i=1}^{N}\sigma_i^{m_v}\ln(\sigma_i)}{\sum_{i=1}^{N}\sigma_i^{m_v}} = 0 \quad (7)$$

$$\sigma_{0v} = \left[\frac{V}{N}\sum_{i=1}^{N}\sigma_i^{m_v}\right]^{1/m_v} \quad (8)$$

A possible bias in the estimator [21, 22] was taken into account. The estimates of statistical parameters were corrected using the following method [21]

$$m = \hat{m}/\frac{\bar{m}_A}{m}$$
$$S_m = mC_{v,m} \quad (9)$$

where $\hat{m}$ is the estimated value of m, m is the corrected value, S_m is the associated standard deviation. $\bar{m}_A/m$ and C_{vm} are, respectively, the estimated means and the standard deviation of the distribution of the estimator of m. They were computed as a function of the sample size, using a Monte Carlo simulation [21]. This method was also applied to obtain bias and standard errors for the values of σ_0.

The fit of the Weibull distribution was assessed using the Andersson–Darling test. The Andersson–Darling statistics called A^2, is defined in the following equation:

$$A^2_n = -N - \frac{1}{N}\sum_{i=1}^{N}(2i - 1)\ln(P_i) + (2n + 1 - 2i)\ln(1 - P_i) \quad (10)$$

A modified formula has been proposed by D'Agostino and Stephens [23] for a Weibull distribution and a finite population of N data

$$A^* = A^2_n(1 + 0.2/N^{1/2}) \quad (11)$$

As an approximate rule, only values of $A^* \leqslant 0.5$ are likely to have meaningful significance.

3. Failure probability equations

The failure probability equations were established for the different flaw populations and for the stress states that were examined in the present paper. The failure probability strength relations in the presence of varying fibre diameters were obtained by incorporating the stress-state description in the following Weibull equation

$$P = 1 - \exp\left[- \int_A \left(\frac{\sigma}{\sigma_0}\right)^m \mathrm{d}A \right] \quad (12)$$

where A refers to the surface or the volume of the fibre. The stress state was derived from the linear variations of the diameter, between the 5 mm apart $2R_i$ and $2R_{i+1}$ values (Fig. 3):

$$\sigma(z) = \frac{F}{\pi R^2(z)} \quad (13a)$$

with

$$R(z) = \frac{z}{l}(R_{i+1} - R_i) + R_i \quad (13b)$$

where l is the distance between R_i and R_{i+1} ($l = 5$ mm).

A convenient form of probability–strength relations uses the equivalent volume, V_E (or an equivalent surface in the presence of surface-located failure origins)

$$P = 1 - \exp\left[- V_E \left(\frac{\sigma_{\max}}{\sigma_{0v}}\right)^{m_v} \right] \quad (14a)$$

where

$$V_E = S \int_0^L \left(\frac{\sigma(z)}{\sigma_{\max}}\right) \mathrm{d}z \quad (14b)$$

S is the cross-sectional area of the fibre, L is the length and $\sigma_{\max}$ is the maximum stress in the fibre. For the uniform stress-state $\sigma(z)/\sigma_{\max} = 1$ and $V_E = V$.

The failure probability–strain to failure, $P - \varepsilon$, relations were given by the following equation for volume-located failure origins (a similar equation is easily obtained for surface-located failure origins)

$$P = 1 - \exp\left[- V \left(\frac{\varepsilon}{\varepsilon_{0v}}\right)^{m_v} \right] \quad (15)$$

The resulting equations of failure probability were then combined to account for the contribution of concurrent or partially concurrent populations of fracture-inducing flaws. For conciseness, equations will be presented only for failure probability–strength relations.

3.1. Failure probability–strength equations in the presence of single flaw population

If the fracture-inducing flaws are assumed to be located in the interior of the fibres, the failure probability–strength relation is given by Equation 14. In the presence of a constant fibre radius, $V_E = V$. In the presence of a variable fibre radius, $\sigma_{\max} = \sigma_{d_{\min}}$ and

$$V_E = \sum_{i=1}^{n-1} \frac{R_{\min}^{2m_v} \pi l}{(3 - 2m_v)(R_{i+1} - R_i)} \times [R_{i+1}^{3-2m_v} - R_i^{3-2m_v}] \quad (16)$$

$R_{\min}$ is the minimum radius observed in the fibre.

3.2. Failure probability–strength relations in the presence of bimodal concurrent flaw populations

Concurrent flaw populations pre-exist simultaneously within all the specimens. In the presence of concurrent surface- and volume-located flaw populations, failure probability is obtained from the product of survival failure probabilities

$$P = 1 - (1 - P_s)(1 - P_v) \quad (17)$$

where P_s and P_v are, respectively, the probabilities of failure from surface- and volume-located flaws. The overall failure probability reduces to

$$P = 1 - \exp\left[- V_E \left(\frac{\sigma_{\max}}{\sigma_{0v}}\right)^{m_v} - S_E \left(\frac{\sigma_{\max}}{\sigma_{0s}}\right)^{m_s} \right] \quad (18)$$

where σ_{0s} and m_s are the statistical parameters for surface-located failure origins. S_E is the effective surface. S_E coincides with the fibre external surface in the presence of a uniform stress state

$$S_E = 2\pi RL \quad (19)$$

In the presence of stress gradients, S_E is given by the following equation

$$S_E = \sum_{i=1}^{n-1} \frac{R_{\min}^{2m_s} 2\pi l}{(2 - 2m_s)(R_{i+1} - R_i)} \times [R_{i+1}^{2-2m_s} - R_i^{2-2m_s}] \quad (20)$$

V_E is given by Equation 16 and $\sigma_{\max} = \sigma_{d_{\min}}$.

Transition of failure origin from surface to volume is characterized by a transition stress, σ^*, and a transition strain, ε^*, such that $P_s = P_v$

$$\sigma^* = \left[\frac{S_E(\sigma_{0v})^{m_v}}{V_E(\sigma_{0s})^{m_s}}\right]^{1/(m_v - m_s)} \quad (21)$$

$$\varepsilon^* = \left[\frac{S_E(\varepsilon_{0v})^{m_v}}{V_E(\varepsilon_{0s})^{m_s}}\right]^{1/(m_v - m_s)} \quad (22)$$

3.3. Failure probability–strength relations in the presence of bimodal partially concurrent flaw populations

Bimodal partially concurrent [24] populations include one family of flaws pre-existing within all the samples (intrinsic flaws), whereas flaws of the second family are present only within certain specimens (extrinsic flaws). Failure probability can be obtained from the following equation

$$P = (1 - \pi_2)P_1 + \pi_2[1 - (1 - P_1)(1 - P_2)] \quad (23)$$

where π_2 is the fraction of specimens containing the extrinsic flaws. P_1 refers to intrinsic flaws and P_2 to the extrinsic flaws. The overall failure probability reduces to

$$P = 1 - (1 - \pi_2)\exp\left[- v_{E1}\left(\frac{\sigma_{max}}{\sigma_{01}}\right)^{m_1}\right] - \pi_2\exp\left[- v_{E1}\left(\frac{\sigma_{max}}{\sigma_{01}}\right)^{m_1} - v_{E2}\left(\frac{\sigma_{max}}{\sigma_{02}}\right)^{m_2}\right] \quad (24)$$

where V_{E1} and V_{E2} are the effective volumes respective to intrinsic and extrinsic flaws.

In the presence of a uniform stress state, $V_{E1} = V_{E2} = V$. In the presence of stress gradients, V_{E1} and V_{E2} are given by Equation 16 for the respective Weibull moduli, m_1 and m_2.

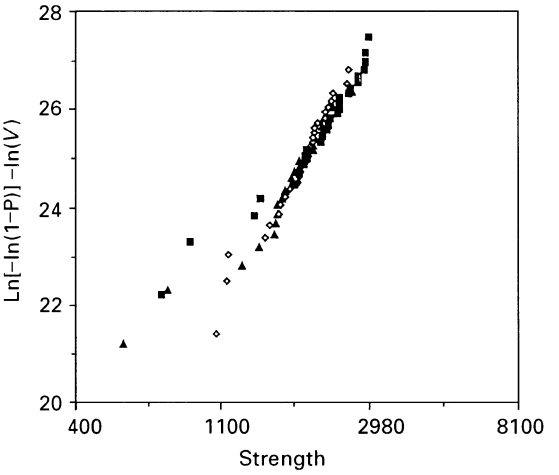

Figure 5 Log plot of Nicalon fibre strengths versus $\ln[1/V(-\ln(1-P)]$ at various gauge lengths: (▲) 25 mm, (◇) 50 mm, (■) 75 mm.

4. Results and discussion

4.1. Failure data

Comparable statistical distributions of failure data were obtained whatever the fibre diameter estimate employed for strength determination (d_{AV}, d_{SEM}, d_{min}) or whatever the failure data selected (stress or strain) (Fig. 4). Inspection of these loglog plots revealed the presence of two distinct families of data at the 25 and 75 mm gauge lengths, whereas a single family was observed for the 50 mm gauge length. Evidence of these trends is also given by the statistical distributions of strains to failure (Fig. 4d) which indicates that the family of failures at the low stresses must not be attributed to an artefact in diameter or failure force measurement.

Fig. 5 shows a statistical distribution of strength data plotted independently of the scale effects induced by gauge lengths. This plot confirms the presence of two distinct families of failure data. Most data fall into a single line, whereas a few data at the low strength extreme suggest the presence of a second population of fracture origins in the 25 and 75 mm gauge length fibres.

SEM examination of fracture surfaces revealed the presence of fracture-inducing flaws located in the surface or in the interior of fibres (Fig. 6). Fracture origins were shown by fracture mirrors. Surface-located fracture origins dominated fracture at the low strengths or strains, whereas volume-located fracture origins were essentially identified in those fibres that failed at higher stresses or strains. Most failure data from surface- and volume-located flaws fall into the main line of Fig. 5. The flaws at the low-strength extremes did not

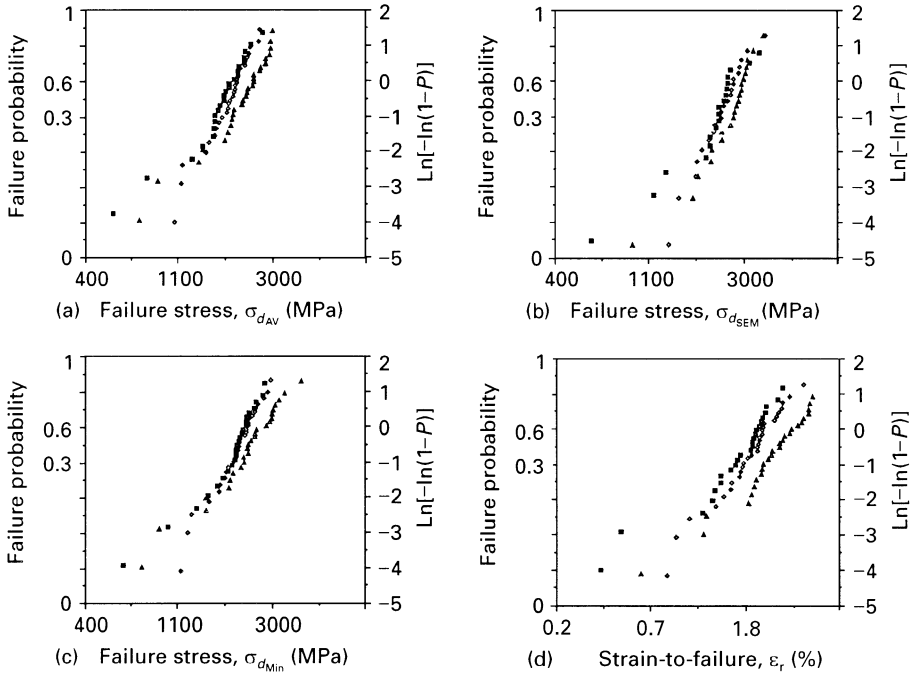

Figure 4 Log log plot of Nicalon fibre data versus cumulative failure probability obtained at various gauge lengths for different estimates of fibre failure: (a) $\sigma_{d_{AV}}$, (b) $\sigma_{d_{SEM}}$, (c) $\sigma_{d_{min}}$ and (d) failure strain, ε_R: (▲) 25 mm, (◆) 50 mm, (■) 75 mm.

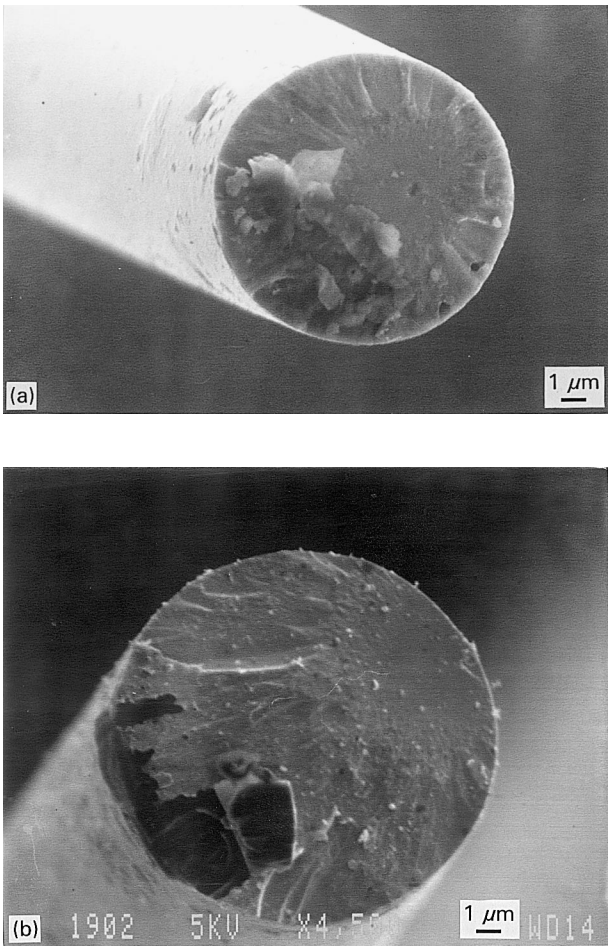

Figure 6 Scanning electron micrographs showing (a) volume- and (b) surface-located fracture origins in Nicalon fibres.

TABLE II Mean strengths $\bar{\sigma}_{d_{AV}}$, $\bar{\sigma}_{d_{SEM}}$ and $\bar{\sigma}_{d_{min}}$ and mean strains-to-failure, $\bar{\varepsilon}_{min}$, for the Nicalon fibres. Standard deviations are given in parentheses

Gauge length (mm)	$\bar{\sigma}_{d_{AV}}$	$\bar{\sigma}_{d_{SEM}}$	$\bar{\varepsilon}_r$ (%)	$\bar{\sigma}_{d_{min}}$
25	2203 (584)	2692 (663)	1 (0.25)	2678 (754)
50	1914 (388)	2263 (634)	0.9 (0.18)	2108 (454)
75	1773 (466)	2100 (624)	0.84 (0.19)	1947 (500)

exhibit any specific geometrical feature which differentiates them from the other surface-located flaws.

Table II shows that $\sigma_{d_{SEM}}$ and $\sigma_{d_{min}}$ are significantly larger than $\sigma_{d_{AV}}$ indicating that failure initiated preferentially in the most narrow sections of fibres. Strengths derived from average fibre diameters are, therefore, underestimated.

Fig. 7 shows that the lowest strength data were obtained with those fibres having the largest diameters. Fig. 7 also clearly indicates that such low strengths cannot be attributed solely to a scale effect induced by the diameter. These results suggest that fracture origins at the low-strength extreme do pertain to a distinct flaw population.

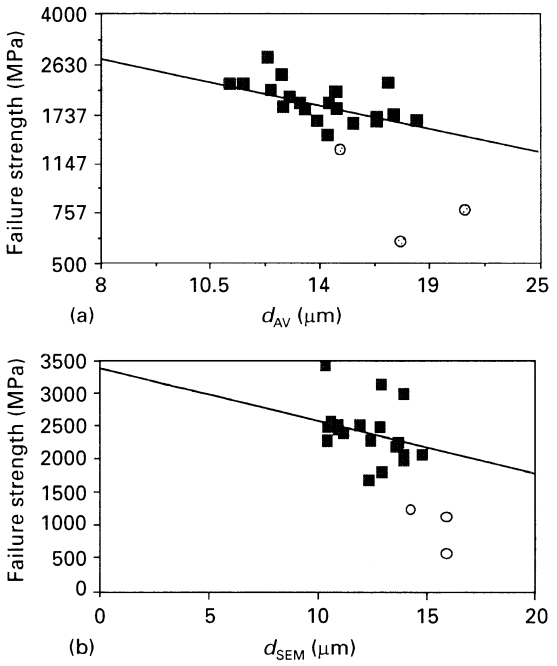

Figure 7 Influence of fibre diameter upon Nicalon fibre strength (gauge length = 75 mm): (a) average diameter measured by laser diffractometry; (b) diameter at fibre location. The solid line shows the theoretical dependence of strength on diameter (slope = $-2/m$), (○) data at low-strength extreme.

Therefore, the fracture-inducing flaws may be grouped into two families:

(i) a family of extrinsic flaws responsible for fracture at the low-strength extremes in the fibres having a 25 or 75 mm gauge length;

(ii) a population of intrinsic flaws present within all the fibres and located in the surface and in the interior of fibres.

To assess the validity of this classification, the distributions of failure data were analysed assuming the previously mentioned possible populations of fracture origins.

4.2. Statistical parameters

4.2.1. Assuming a single flaw population

A significant dependence of statistical parameters estimates on gauge length, the estimator and the failure data considered, may be observed in Tables III and IV. Andersson–Darling parameter, A^*, is smaller than 0.5 only for the 50 mm gauge length. A^* is also smaller than 0.5 at the 25 mm gauge length for the maximum likelihood estimates. These results indicate that a Weibull distribution may not be accepted because it was found inappropriate for the 75 mm gauge length ($A^* > 0.6$).

A smaller scatter was observed with the statistical parameters estimated using the maximum likelihood estimator. This result is in agreement with logical expectation, because maximum likelihood estimates are generally less influenced by data at the extremes of distributions than are the parameters estimated using linear regression. It is worth pointing out that the narrowest scatter was observed with the distributions of strains-to-failure.

TABLE III Statistical parameters estimated by linear regression method for the Nicalon fibres, assuming the presence of a single population of fracture-inducing flaws

Gauge length (mm)		m_v	Standard deviation	σ_{0v} (MPam$^{3/m_v}$) ε_{0v} (m^{3/m_v})	Standard deviation	A^*
25	$\sigma_{d_{AV}}$	3.5	0.68	1.38	0.05	0.76
	$\sigma_{d_{SEM}}$	3.85	0.74	4.07	0.04	0.70
	$\sigma_{d_{min}}$	3.2	0.64	0.57	0.063	0.5
	ε_r	4.44	0.86	3.33×10^{-5}	1.34×10^{-6}	0.65
50	$\sigma_{d_{AV}}$	5.46	1	19.55	0.81	0.34
	$\sigma_{d_{SEM}}$	4.91	0.95	14.46	0.58	0.33
	$\sigma_{d_{min}}$	5.46	1	12.78	0.81	0.2
	ε_r	5.55	1	1.02×10^{-4}	4×10^{-6}	0.33
75	$\sigma_{d_{AV}}$	3.47	0.68	1.43	0.06	0.97
	$\sigma_{d_{SEM}}$	3.13	0.61	0.9	0.03	1.07
	$\sigma_{d_{min}}$	3.55	0.69	1.075	0.07	1.18
	ε_r	3.98	0.78	1.76×10^{-5}	7.4×10^{-7}	1.16

TABLE IV Statistical parameters estimated by maximum likelihood method for the Nicalon fibres, assuming the presence of a single population of fracture-inducing flaws

Gauge length (mm)		m_v	Standard deviation	σ_{0v} (MPam$^{3/m_v}$) ε_{0v} (m^{3/m_v})	Standard deviation	A^*
25	$\sigma_{d_{AV}}$	4.65	0.7	8.54	0.34	0.45
	$\sigma_{d_{SEM}}$	4.96	0.76	14.8	0.62	0.58
	$\sigma_{d_{min}}$	3.65	0.57	1.58	0.06	0.4
	ε_r	5.19	0.79	7.61×10^{-5}	3.13×10^{-6}	0.31
50	$\sigma_{d_{AV}}$	5.97	0.87	28.61	1.1	0.29
	$\sigma_{d_{SEM}}$	5.14	0.8	17.77	0.73	0.31
	$\sigma_{d_{min}}$	5.46	0.8	15.87	0.61	0.19
	ε_r	5.81	0.85	1.23×10^{-4}	4.7×10^{-4}	0.27
75	$\sigma_{d_{AV}}$	4.62	0.71	8.43	0.35	0.56
	$\sigma_{d_{SEM}}$	4.12	0.66	5.39	0.23	0.67
	$\sigma_{d_{min}}$	5.11	0.81	10.2	0.408	0.60
	ε_r	5.16	0.80	1.02×10^{-4}	5.4×10^{-6}	0.68

Maximum likelihood estimates were larger than those obtained by linear regression. Both sets of estimates were close only for the 50 mm gauge length, which is in agreement with logical expectation.

4.2.2. Assuming concurrent populations

The distributions of failure data were separated to conform with the presence of concurrent populations of surface- and volume-located flaws (Fig. 8). The censored data method proposed by Johnson was employed [25]. This method determines a new rank, i', for the data of each population by calculating a new increment, Δ, as soon as one or more censored data of the other population are encountered in the sequence of test data.

Tables V and VI show that the sensitivity of statistical parameters estimates to the previously mentioned factors is reduced, and that the Andersson–Darling parameters, A^*, are now smaller than previously. Most of the previous conclusions apply. Let us just point out the most important. The Andersson–Darling test shows that only the data obtained for a 50 mm gauge length may be described using a Weibull distribution. However, it can be seen that a Weibull distribution may be regarded as quite

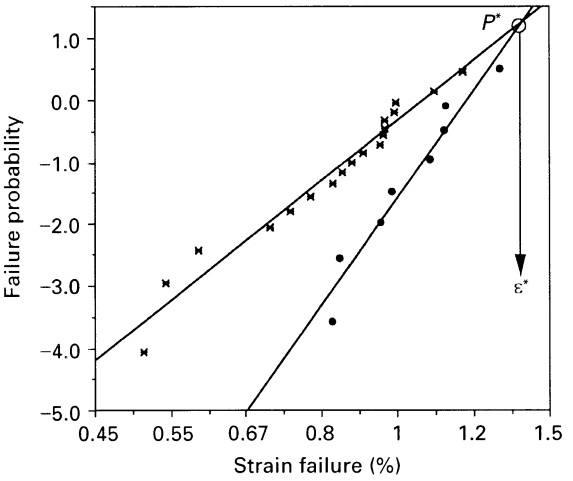

Figure 8 Log log plot of the separated distribution of failure strain data obtained for concurrent (∗) surface- and (●) volume-located flaw populations.

TABLE V Statistical parameters for Nicalon fibres estimated by the linear regression method, assuming the presence of concurrent populations of surface- and volume-located populations of flaws. Standard deviations are given in parentheses

	$L = 25$ mm					$L = 50$ mm					$L = 75$ mm				
	m_s	σ_{0s}	m_v	σ_{0v}	A^*	m_s	σ_{0s}	m_v	σ_{0v}	A^*	m_s	σ_{0s}	m_v	σ_{0v}	A^*
$\sigma_{d_{AV}}$	2.96	28	6.85	65	0.57	4.48	127	8.63	123	0.36	2.98	32	6.14	40	0.72
	(0.69)*	(1.42)	(2.66)	(5.27)		(1)*	(6.46)	(3)	(10)		(0.69)*	(1.63)	(2.5)	(3.5)	
$\sigma_{d_{SEM}}$	3.5	77	6.3	54	0.52	4.45	151	6.03	47	0.32	2.88	33	4.08	6.77	1
	(0.23)	(3.9)	(2.45)	(4.38)		(1)	(7.69)	(2)	(3.81)		(0.67)	(1.68)	(1.7)	(0.6)	
$\sigma_{d_{min}}$	2.87	18.43	5.45	25.68	0.55	4.32	80	7.42	64.65	0.3	3.03	20.35	6.47	39.03	0.92
	(0.66)	(1.5)	(2.31)	(2.03)		(1)	(4)	(2.87)	(5.5)		(0.72)	(2.86)	(2.48)	(2.34)	
		ε_{0s}		ε_{0v}			ε_{0s}		ε_{0v}			ε_{0s}		ε_{0v}	
ε_r	3.84	3.8×10^{-4}	6.94	3.3×10^{-4}	0.46	4.8	2×10^{-4}	8.6	6.2×10^{-4}	0.38	3.26	2×10^{-4}	7.6	4×10^{-4}	0.98
	(0.89)	(2×10^{-5})	(2.7)	(2.6×10^{-5})		(1.12)	(1×10^{-5})	(2.9)	(5×10^{-5})		(0.76)	(1×10^{-5})	(3)	(3.6×10^{-5})	

TABLE VI Statistical parameters for Nicalon fibres estimated by the maximum likelihood method, assuming the presence of concurrent populations of surface- and volume-located populations of flaws. Standard deviations are given in parentheses

	$L = 25$ mm					$L = 50$ mm					$L = 75$ mm				
	m_s	σ_{0s}	m_v	σ_{0v}	A^*	m_s	σ_{0s}	m_v	σ_{0v}	A^*	m_s	σ_{0s}	m_v	σ_{0v}	A^*
$\sigma_{d_{AV}}$	3.5	71.64	6.72	50.3	0.51	4.75	162	7.86	86	0.31	4.45	135	5.5	22.6	0.42
	(0.66)*	(3.7)	(2)	(4.13)		(0.9)	(8.14)	(2.2)	(6.3)		(0.84)	(6.79)	(1.8)	(1.99)	
$\sigma_{d_{SEM}}$	4.3	128	8	143	0.46	4.3	152	5.1	19	0.31	4.2	157	5.47	27	0.68
	(0.81)	(6.4)	(2.5)	(11.8)		(0.81)	(7.64)	(1.43)	(1.4)		(0.8)	(7.8)	(1.78)	(2.38)	
$\sigma_{d_{min}}$	3.47	34.77	4.85	48	0.6	4.67	88.49	7.09	48.75	0.24	5.34	118.2	6.25	29.58	0.56
	(0.57)	(1.81)	(1.46)	(3.92)		(0.79)	(4)	(2.14)	(3.43)		(1)	(0.62)	(1.89)	(2.41)	
		ε_{0s}		ε_{0v}			ε_{0s}		ε_{0v}			ε_{0s}		ε_{0v}	
ε_r	4.68	6.2×10^{-4}	7	2.8×10^{-4}	0.49	5.28	9.6×10^{-4}	7.45	3.6×10^{-4}	0.29	5.13	9×10^{-4}	7.35	3×10^{-4}	0.62
	(0.88)	(3×10^{-5})	(2.1)	(2.3×10^{-5})		(1)	(4.8×10^{-5})	(2)	(2.6×10^{-5})		(0.97)	(4.52)	(2.4)	(2.64×10^{-5})	

satisfactory when considering the maximum likelihood estimates derived from the $\sigma_{d_{AV}}$ data. Again it is worth pointing out that the narrowest scatter was observed with the strain-to-failure data.

The larger statistical parameters were obtained for the volume-located flaws. These parameters exhibit a significant scatter, except when considering the strain data. This scatter may be related to the sample size, because only 20%–30% of the failures were initiated by volume-located flaws.

Because the Andersson–Darling test is not usually applied in the presence of bimodal populations of data, in order to assess the above conclusions the probability-strength relations were computed for the statistical parameters estimated from the $\sigma_{d_{AV}}$ data (Tables V and VI). Computations were then compared to the corresponding experimental strength distributions (Fig. 9). The results confirm that an excellent fit is obtained only with the strength data measured at a 50 mm gauge length. For the other gauge lengths, agreement between computed and experimental data is poor at the low-strength extremes. These results substantiate the use of low values of $A^* < 0.5$ as a criterion of goodness of fit in the presence of bimodal populations.

The transition strengths, σ^*, and deformations, ε^*, were determined from the intersection of the distributions of failure data pertinent to the surface- and volume-located failure origins (Fig. 8). The results agree satisfactorily well with σ^* and ε^* computed using Equations 21 and 22 (Table VII). σ^* and ε^* are rather high when compared with the mean values of strengths and strains-to-failure (Table II) which reflects the dominance of surface-located flaws in fibre failure as evidenced by SEM fractography. Table VII also shows that σ^* and ε^* decrease with increasing gauge lengths, as a result of correlative increases in volume contribution according to the relation $V/S = L$.

4.2.3. Assuming partially concurrent populations

The Andersson–Darling parameters are now smaller than previously and they are below 0.5, indicating that Weibull statistics describe satisfactorily the distributions of failure data (Tables VIII and IX). The statistical parameters estimated by linear regression show a limited sensitivity to gauge length. In particular it is worth noting that the estimates of parameters pertinent to the intrinsic flaws are very close. The smallest scatter in estimates was observed for the strains-to failure. The scatter in the maximum likelihood estimates was the larger. However, the Andersson–Darling test indicates a better goodness-of-fit of the Weibull distribution to the experimental data with these latter estimates. All these results strongly substantiate the validity of separating the data into two partially concurrent populations of extrinsic and intrinsic flaws.

TABLE VII Comparison of transition strengths, σ*, and strains, ε*, computed using Equations 21 and 22 with experiemental data for various gauge lengths

	Experimental data			Theoretical data		
	25 mm	50 mm	75 mm	25 mm	50 mm	75 mm
$\sigma_{d_{AV}}$	2980	2565	2835	3100	2439	2612
$\sigma_{d_{SEM}}$	3640	3463	3314	3055	4100	3810
$\sigma_{d_{min}}$	4000	3133	2835	3760	3100	2917
ε_r	1.6	1.4	1.1	1.7	1.4	1.1

The Andersson–Darling test also indicates a comparable goodness-of-fit when the statistical parameters are estimated from either the $\sigma_{d_{min}}$ or the $\sigma_{d_{SEM}}$ or the $\sigma_{d_{AV}}$ data. Diameter variations along the fibre axis do not significantly influence the results. Similar estimates of Weibull parameters were obtained indicating that the distribution of $\sigma_{d_{AV}}$ data is appropriate for statistical parameters determination.

Using strains as failure data appears to be the most satisfactory solution. The Andersson–Darling parameter was the smallest in most cases and a limited scatter in statistical parameter estimates was observed, showing a slight sensitivity to gauge length. Using strain data is very convenient because there is no need to measure fibre diameters.

4.3. Predictions at various gauge lengths

In order to assess the validity of the above analysis, probability–failure strain or stress relations at various gauge lengths were predicted from the statistical parameters determined for the 25 mm gauge length. The estimates displaying a limited scatter and providing a good fit as indicated by the Andersson–Darling test were selected:

(i) the parameters estimated by maximum likelihood method from the distribution of strains to failure, assuming the presence of two concurrent populations of surface- and volume-located flaws (Table VI),

(ii) the parameters estimated by linear regression method from the distribution of $\sigma_{d_{AV}}$ data, assuming the presence of two partially concurrent populations of extrinsic and intrinsic flaws (Table VIII).

Failure probabilities were computed using Equations 17 and 24, respectively.

Figs 10 and 11 compare predictions with experimental data. Predictions visually agree fairly well with experimental data. However a better fit is observed in Fig. 11, particularly at the low-strength extremes. Again this result supports the separation of failure data into two families involving partially concurrent intrinsic and extrinsic flaws. The results also confirm that the distributions of $\sigma_{d_{AV}}$ strength data provided satisfactory estimates of the statistical parameters for prediction purposes. They show that linear regression

TABLE VIII Statistical parameters for Nicalon fibres estimated by the linear regression method, assuming the presence of partially concurrent flaw populations. Standard deviations are given in parentheses

	$L = 25$ mm					$L = 50$ mm					$L = 75$ mm				
	m_1	σ_{01}	m_2	σ_{02}	A^*	m_1	σ_{01}	m_2	σ_{02}	A^*	m_1	σ_{01}	m_2	σ_{02}	A^*
$\sigma_{d_{AV}}$	5.13	14.7	2.29	0.04	0.38	5.46	19.5			0.34	5.45	19.5	1.92	7×10^{-3}	0.34
	(1.11)*	(0.66)	(1.16)	(4.2×10^{-3})		(1)	(0.81)				(1.2)	(0.93)	(0.97)	(7.4×10^{-4})	
$\sigma_{d_{SEM}}$	5.24	19.5	2.14	0.027	0.42	4.91	14.49			0.33	4.81	13.31	1.99	0.013	0.56
	(1)	(0.93)	(1.1)	(2.8×10^{-3})		(0.95)	(0.58)				(1)	(0.63)	(1)	(1.3×10^{-3})	
$\sigma_{d_{min}}$	5.48	20	2.2	0.017	0.39	5.22	12.78			0.20	5.69	31.10	2.26	0.026	0.38
	(1.17)	(0.69)	(1.1)	(2.3×10^{-3})		(0.98)	(0.8)				(1.25)	(0.9)	(1.07)	(1.7×10^{-3})	
		ε_{01}		ε_{02}			ε_{01}					ε_{01}		ε_{02}	
ε_r	5.64	1.1×10^{-4}	3.12	3.4×10^{-6}	0.24	5.5	1×10^{-4}			0.33	6.16	1×10^{-4}	2.04	8×10^{-8}	0.27
	(1.21)	(5×10^{-6})	(1.59)	(3.6×10^{-7})		(1.03)	(4×10^{-6})				(1.34)	(4.8×10^{-6})	(1)	(8×10^{-9})	

TABLE IX Statistical parameters for Nicalon fibres estimated by maximum likelihood method, assuming the presence of partially concurrent populations of flaws. Standard deviations are given in parentheses

	$L = 25$ mm					$L = 50$ mm					$L = 75$ mm				
	m_1	σ_{01}	m_2	σ_{02}	A^*	m_1	σ_{01}	m_2	σ_{02}	A^*	m_1	σ_{01}	m_2	σ_{02}	A^*
$\sigma_{d_{AV}}$	6.63	48.2	3.85	1.2	0.31	5.97	28.6			0.28	6.37	40	3.15	0.32	0.38
	(1.09)	(2.16)	(1.42)	(0.13)		(0.87)	(1.1)				(1)	(1.84)	(1.16)	(0.034)	
$\sigma_{d_{SEM}}$	6.31	47.6	4.75	6.54	0.44	5.14	17.73			0.30	5.88	35	3.65	0.98	0.59
	(1)	(2.19)	(1.7)	(0.7)		(0.8)	(0.73)				(1)	(1.62)	(1.34)	(0.1)	
$\sigma_{d_{min}}$	4.95	12.59	3.45	0.38	0.34	5.46	15.87			0.24	8	76.15	3.6	0.68	0.4
	(0.84)	(0.52)	(1.27)	(3.2×10^{-2})		(0.8)	(0.61)				(1.45)	(3.7)	(1.33)	(0.01)	
		ε_{01}		ε_{02}			ε_{01}					ε_{01}		ε_{02}	
ε_r	6.98	3×10^{-4}	4.47	3×10^{-6}	0.34	5.81	1.2×10^{-4}			0.26	7.85	3.9×10^{-4}	3.21	2.6×10^{-6}	0.21
	(1.15)	(1.4×10^{-6})	(1.65)	(3.2×10^{-7})		(0.85)	(4.7×10^{-6})				(1.342)	(1.8×10^{-5})	(1.18)	(2.6×10^{-7})	

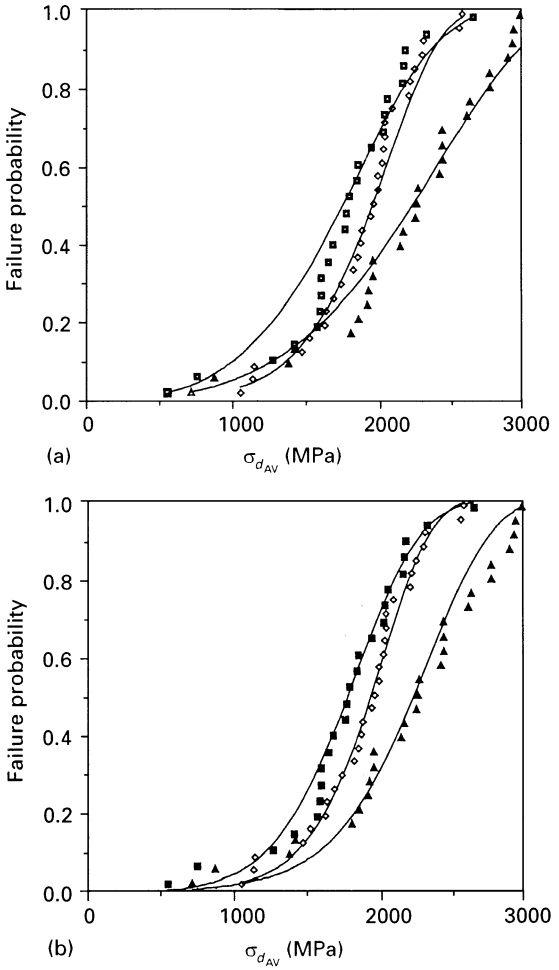

Figure 9 Comparison of the experimental strength distributions for Nicalon fibre at various gauge lengths and the Weibull distributions computed assuming concurrent flaw populations (Equation 18). The statistical parameters have been estimated by (a) linear regression and (b) maximum likelihood methods: (▲) 25 mm, (◇) 50 mm, (■) 75 mm.

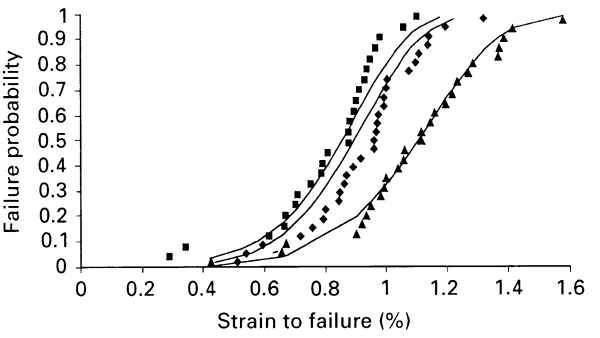

Figure 10 Comparison of the experimental distributions of Nicalon fibre strains to failure at various gauge lengths and predictions from the statistical parameters estimated for a 25 mm gauge length using maximum likelihood method (concurrent populations of surface- and volume-located flaws): (▲) 25 mm, (◆) 50 mm, (■) 75 mm.

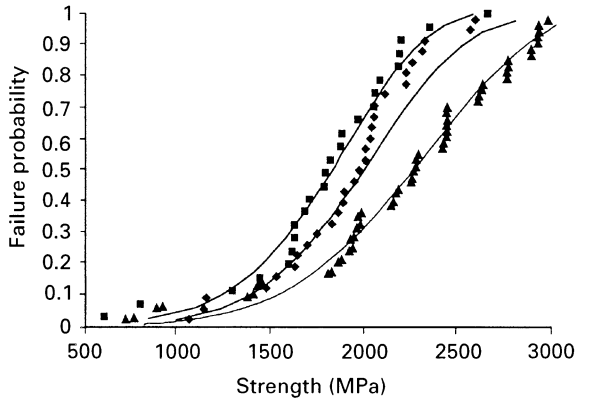

Figure 11 Comparison of the experimental distribution of Nicalon fibre strengths at various gauge lengths and predictions from the statistical parameters estimated for a 25 mm gauge length using the linear regression method (partially concurrent populations of flaws): (▲) 25 mm, (◆) 50 mm, (■) 75 mm.

method is appropriate for statistical parameters estimation, provided fracture origins are properly identified and failure data are separated accordingly.

4.4. Evaluation of the influence of uncertainty in the statistical parameters m and σ_0:

Uncertainty in failure probability computations was obtained by performing the differentiation of the failure probability equation, taking into account the dependence of σ_0 upon m (Equation 8)

$$dP = \left[\left(\frac{\partial P}{\partial m}\right) + \left(\frac{\partial P}{\partial \sigma_0}\right)\left(\frac{\partial g}{\partial m}\right)\right] dm \qquad (25)$$

Inserting the derivative of Equation 8 into Equation 12, failure probability uncertainty reduces to a function of the uncertainty in m

$$\frac{\Delta P}{1 - P} = \Delta m V \left(\frac{\sigma}{\sigma_0}\right)^m \left[\ln(\sigma) - \frac{\sum_{i=1}^{N} \ln(\sigma_i)\sigma_i^m}{\sigma_0^m V/N}\right] \qquad (26)$$

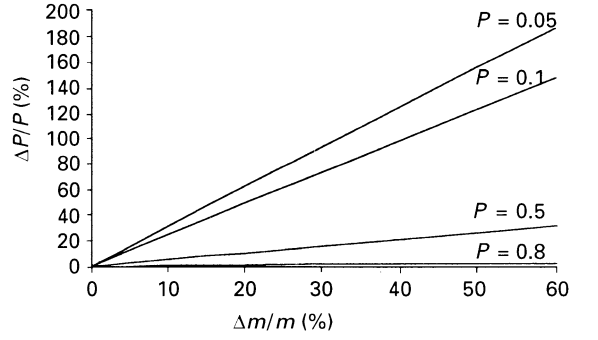

Figure 12 Uncertainty in failure probability as a function of the uncertainty in Weibull modulus given by Equation 26 for various failure probabilities.

Fig. 12 shows the influence of the uncertainty in m on the failure predictions. The dependence of failure probability computations upon m uncertainty increases with decreasing failure probabilities.

The uncertainty observed on the m estimates comprised between 5% and 50%. The large uncertainty was induced by the populations of volume-located or extrinsic flaws. The corresponding uncertainty in failure probability varies between 2% and 25% for a 50% failure probability, and between 12–25% and 123%

for a 10% failure probability. The predictions of failures at the low-strength extremes are very sensitive to the Weibull modulus. Therefore, a significant effort in the estimation of the true statistical parameters is required.

5. Conclusion

The distributions of failure data including strains-to-failure or strength for SiC fibres may not be described solely in terms of the two-parameter Weibull function, owing to the presence of bimodal populations of fracture-inducing flaws. In the present work, this effect was attributed to the presence of two partially concurrent flaw populations including extrinsic flaws located in the surface and intrinsic flaws located both in the surface and in the volume. The extrinsic flaws exhibit a similar geometry but a higher severity when compared with intrinsic surface-located flaws. The exact nature of these flaws has not yet been identified. However, data suggest that the contribution of these flaws to fibre failure may be related to the presence of samples with a larger diameter.

This separation of flaws into two partially concurrent populations was assessed by comparing the estimates of the statistical parameters obtained when assuming the presence of three possible flaw populations. The Andersson–Darling test showed that the best fit of the distributions to the experimental data is obtained when assuming the presence of partially concurrent populations of flaws, whatever the method of estimating the statistical parameters. This result was confirmed by the predictions of distributions at various gauge lengths from the statistical parameters estimated at the shortest gauge. The best results were obtained when using strains as failure data. Strain is very convenient because there is no need to measure fibre diameter. However, using the average fibre diameter for strength evaluation may provide satisfactory approximation for failure prediction purposes.

Poorer results were obtained when considering a single population of flaws or two concurrent populations of surface- and volume-located flaws. In both cases, the Andersson–Darling test showed that the failure data cannot be properly described using Weibull statistics, as a result of the presence of failure data at the low-strength extreme. An improvement was observed with the maximum likelihood estimates, based upon $\sigma_{d_{AV}}$ and in the presence of concurrent flaw-populations. In this latter case, the highest value observed for the Andersson–Darling parameter was 0.51, indicating that a Weibull distribution may be regarded as sound. This latter result perfectly highlights the discrepancy that may exist between purely statistical approaches and physical foundation of failure.

The maximum likelihood estimator is generally preferred due to its small bias error in the presence of low-strength extremes. However, it was shown that the linear regression estimator is capable of providing satisfactory estimates of statistical parameters for prediction purposes, provided the populations of fracture inducing flaws are properly considered. In summary, the following statistical parameters seem to be appropriate for the SiC Nicalon fibres: $m_1 = 5.5$, $\sigma_{01} = 19$ MPa (intrinsic failures); $m_2 = 2$, $\sigma_{02} = 0.02$ MPa (extrinsic failures), both with reference volume $V_0 = 1\ m^3$.

Acknowledgements

The authors acknowledge the support of CNRS and SEP which allowed completion of this research work.

References

1. W. WEIBULL, *R. Swedish Acad. Eng. Sci. Proc.* **151** (1939) 1.
2. G. SIMON and A. R. BUNSELL, *J. Mater. Sci.* **19** (1984) 3649.
3. C. H. ANDERSSON and R. WARREN, in "Advances in Composite Materials", Vol 2, ICCM3, edited by A. R. Bunsell (Pergamon Press, Paris, 1980) pp. 1129–39.
4. D. B. FISCHBACH, P. M. LEMOINE and G. V. YEN, *J. Mater. Sci.* **23** (1988) 987–93.
5. EL. M. ASLOUN, J. B. DONNET, G. GUILPAIN, M. NARDIN and J. SCHULTZ, *ibid.* **24** (1989) 3504–10.
6. A. J. ECKEL and R. C. BRADT, *J. Am. Ceram. Soc.* **72** (1989) 455.
7. J. LAMON, "Mécanique de la rupture des torons de fibres Nicalon: Approche Probabiliste-Statistique", in Comptes rendus des septièmes Journées Nationales sur les Composites, edited by G. Fantozzi and P. Fleischmann, (AMAC, Paris, 1990) pp. 337–350.
8. V. LAVASTE, Thèse, École-Nationale Supérieure des Mines de Paris (1993).
9. K. GODA and H. FUKUNAGA, *J. Mater. Sci.* **21** (1986) 4475.
10. C. P. BEETZ, *Fibre Sci. Technol.* **16** (1982) 45.
11. K. K. PHANI, *J. Mater. Sci.* **23** (1988) 2424.
12. A. S. WATSON and R. L. SMITH, *ibid.* **20** (1985) 3260.
13. S. L. PHOENIX, P. SCHWARTZ and H. H. ROBINSON, *Compos. Sci. Technol.* **32** (1988) 81.
14. C. A. JOHNSON and W. T. TUCKER, "Weibull estimators for fracture data", Life predictions methodologies and data for ceramic materials, ASTM STP 1201, edited by C. R. Brinkman and S. F. Duffy (American Society for Testing and Materials, Philadelphia, PA, 1994) pp. 265–79.
15. J. LAMON, *ibid.*, pp. 175–91.
16. B. BERGMAN, *J. Mater. Sci. Lett.* **4** (1985) 1143.
17. M. LEON and P. KITTL, *J. Mater. Sci.* **20** (1985) 3778.
18. T. W. ANDERSSON and D. A. DARLING, *Ann. Math. Stat.* **22** (1952) 193.
19. J. D. SNEDDEN and C. D. SINCLAIR, in "Mechanics of creep brittle materials-1", edited by A. C. F. Cocks and A. R. S. Ponter (Elsevier Applied Science, 1988), pp. 99–116.
20. CHI-TANG LI and J. V. TIETZ, *J. Mater. Sci.* **25** (1990) 4694.
21. K. TRUSTUM and A. DE S. JAYATILAKA, *ibid.* **14** (1979) 1080.
22. B. BERGMAN, *J. Mater. Sci. Lett.* **3** (1984) 689.
23. R. B. D'AGOSTINO and M. A. STEPHENS, "Goodness of fit techniques" (Marcel Dekker, New York, 1986).
24. C. A. JOHNSON, in "Fracture mechanics of ceramics", Vol. 5, edited by R. G. Bradt, A. G. Evans, D. PH. Hasselman and F. F. Lange (Plenum, New York, 1981) pp. 365–85.
25. L. G. JOHNSON, "The statistical treatment of fatigue experiments" (Elsevier, New York, London, 1964) pp. 37–46.

Received 6 February
and accepted 19 September 1995